e-J. Surf. Sci. Nanotech. Vol. 14 (2016) 225-230 Conference - AsiaNANO 2016 -

Effect of Protein Adsorption on Alignment of Human Gingival Fibroblasts on Grooved Composite Resin*

Tsukasa Akasaka,† Takuya Imamura, Hirofumi Miyaji, Naoyuki Kaga, Atsuro Yokoyama, and Yasuhiro Yoshida
Graduate School of Dental Medicine, Hokkaido University,
Kita 13 Nishi 7, Kita-ku, Sapporo 060-8586, Japan
(Received 31 October 2016; Accepted 21 November 2016; Published 10 December 2016)

Groove patterns on the surface of implants act as an effective barrier to the apical migration of epithelial attachment, after which the grooves facilitate gingival fibroblast attachment. Cell alignment on grooves is largely influenced by the adsorbed protein type. However, cell attachment and cell alignment properties of micro/nano-grooved dental composite resins using osteoblasts and fibroblasts have not been investigated. Further, the effect of saliva-related protein adsorption has not investigated. In this study, we prepared composite resins with grooves that were 2 μm, 1 μm, and 500 nm wide and estimated the effect of pre-coating of some proteins, mainly mucin, on attachment and alignment of human gingival fibroblasts(HGF).

In the cell attachment assay on mucin-coated grooves, the number of attached cells on mucin-coated planar or grooved composite resins was lower compared to that on both composite resins without pre-coating of mucin. Interestingly, the number of attached cells on grooves pre-coated with mucin was 5.7-fold higher than those on planar pre-coated with mucin. Grooves at the micro/nano level may act as a hook for floating cells during the cell attachment assay. Furthermore, the degree of cell alignment was strongly dependent on the pre-coating protein types. The cells were radially spread or round-shaped, but not have sufficient alignment on non-, mucin-, and albumin-coated grooves. Although the cells were attached on the grooves, they were not aligned along the direction of grooves. The cells on fetal bovine serum- or fibronectin-coated grooves exhibited good alignment in the groove direction, particularly on fibronectin-coated grooves. Thus, our patterning method creates an effective seal between soft tissue and dental materials to protect against microorganism invasion.
[DOI: 10.1380/ejssnt.2016.225]

Keywords: Biophysics, medical physics, and biomedical engineering; Surface structure, morphology, roughness, and topography; Biological aspects of nano-structures; Dental composite resin; Human gingival fibroblast

I. INTRODUCTION

Micro/nano-scaled patterning of the surface of dental implants has been investigated to improve adhesion with soft tissue or to connect to bone. Titanium implants with micro grooves (Laser-Lok; BioHorizons, Atlanta, GA, USA) promote the attachment of fibroblasts and osteoblasts and improve soft-tissue attachment or osseointegration because of the specific micro-textured groove patterns on the titanium surface [1, 2]. The repeated groove patterns on the implant surface act as an effective barrier to the apical migration of epithelial attachment and facilitate gingival fibroblast attachment. Grooved patterning has been applied to the surface of some dental materials containing zirconia [3], silica [4], and alumina [5] to control cellular responses.

Micro/nano-scaled groove structures have been shown to cause many cell types to align along the direction of grooves [6]. The percentage of cell alignment on grooves largely increased in the presence of fetal bovine serum(FBS) or fibronectin in the culture medium [7–9]. The adsorption of adhesive molecules or extracellular matrix on the grooves is considered to be critical. Thus, cell alignment on grooves is largely influenced by the adsorbed protein type. However, the effect of adsorption of saliva-related proteins on grooved dental materials on cell alignment has not been examined in detail.

Dental composite resins are mixtures of acrylic resin and filler particles used as restorative materials to repair defects in teeth. In adhesive systems, composite resin is filled into the cavity of teeth and then light-cured. Some researchers have investigated the cell attachment properties of dental composite resins using fibroblasts or osteoblasts [10, 11] because their biocompatibility enables the reformation of normal tissue attachment between dental material surface and gingival connective tissue. However, saliva adsorption on composite resin during dental treatment sometimes occurs, causing saliva contamination and weakening the adhesive bond strength between the composite resin and tooth [12].

Microbial adhesion to the tooth occurs via salivary pellicle formation on the tooth [13]. Recently, in a study by Frenzel *et al.*, dental composite resins were patterned to estimate the effect of saliva-coated surface microstructures on microbial adhesion properties [14]. Their results showed that the microstructures, which were cubes, linear trapezoid, and flat pyramids, of flowable composite surfaces significantly increased the adhesion of oral bacteria compared to that reported for a flat surface. They observed differences in the number of attached bacteria according to the size and type of the microstructures.

Effective attachment or alignment of gingival fibroblasts to grooved composite resins in the intraoral environment occurs through adherence to soft tissue or blocks invading bacteria. However, cell attachment and cell alignment to micro/nano-grooved composite resins using osteoblasts and fibroblasts have not been investigated. Further, the effect of saliva-related protein adsorption has not investigated. In this study, we prepared composite resins with grooves that were 2 μm, 1 μm, and 500 nm wide and estimated the effect of pre-coating of some proteins, mainly mucin, on attachment and alignment of hu-

* This paper was presented at the 8th Asian Conference on Nanoscience and Nanotechnology (AsiaNANO 2016), Sapporo Convention Center, Sapporo, Japan, October 10-13, 2016.
† Corresponding author: akasaka@den.hokudai.ac.jp

man gingival fibroblasts(HGF). We used easily obtainable mucin rather than saliva.

II. EXPERIMENTAL

A. Preparation of grooved composite resins by light-curing

The silicon master molds were purchased from Kyodo International, Inc. (Kawasaki, Japan). The three areas of 5×5 mm^2 used in this study were patterned with grooves/ridges with widths of 2 μm, 1 μm, and 500 nm and a height of 1 μm. Replicas of the master molds were prepared by heat-pressing on a glycol-modified polyethylene terephthalate film (G-PET; Sawada Platec Co., Ltd., Saitama, Japan) with the silicon master mold using a compact heating press (AH-1TC, ASONE corp., Osaka, Japan) at 105°C for 4 min under a pressure of 2 MPa. Grooved composite resins at the micro/nano level were prepared according to the method for micro-structuring of light-curing flowable composite resin with silicone template reported by Frenzel [14]. First, a micro cover glass (thickness No. 5, 24×24 mm^2, Matsunami Glass Ind., Ltd., Osaka, Japan) was treated with ceramic primer (GC Corp., Tokyo, Japan). The ceramic primer was applied for 20 s, and then excess primer was wiped and removed. Approximately 100 mg of flowable composite resin paste (Estelite flow quick; Tokuyama Dental Corp., Tokyo, Japan) was applied to the cover glass. Subsequently, the G-PET replica mold (20×20 mm^2) was added and pressed with a 5-mm transparent acrylic block with a smooth surface. Light-curing was carried out for 20 s by an LED light curing unit (JetLite 5000, J. Morita Corp., Tokyo, Japan). To evaluate the effect of irradiation time, composite resins were light-cured for 5, 10, 20, or 40 s. The resulting grooved composite resin was carefully peeled off from the G-PET mold. Prior to the cell attachment assay, the grooved composite resin was fixed on a tissue culture dish and sterilized under UV irradiation for 4 min.

B. Characterization of the surface of grooved composite resins

Prior to scanning electron microscope (SEM) imaging, the grooved composite resin was coated with Pt-Pd using a sputtering apparatus (E-1030; Hitachi High-Tech Fielding Corp., Tokyo, Japan). The surface morphology of the grooves was observed using SEM (S-4000; Hitachi High-Tech Fielding Corp., Tokyo, Japan). The surface topography and roughness of the sputtered groove was analyzed with a 3D laser scanning confocal microscope (VK-X200; Keyence Corp., Osaka, Japan). The average surface roughness(R_a) was measured on six grooved areas (10×10 μm^2/field). The R_a roughness parameter was calculated as the mean ± standard error based on the standard defined in JIS B0601:2001 (Japanese Industrial Standards, No. B0601).

C. Cell attachment assay of HGF on pre-coated grooves

To estimate the cell attachment ability to patterned composite resin using HGFs (Cosmo Bio Co., Ltd., Tokyo, Japan), we carried out modified cell adhesion testing as previously reported [15, 16]. Briefly, the grooves in a 3.5-cm tissue culture dish were pre-coated with 2 mL of Dulbecco's modified Eagle's medium (DMEM; Sigma-Aldrich, St. Louis, MO, USA) containing mucin (mucin from bovine submaxillary glands, Sigma-Aldrich), FBS (CELLect^{TM} Silver; MP Biomedicals, Solon, OH, USA), fibronectin (0.1% fibronectin solution, from bovine plasma, Sigma-Aldrich), or albumin (BSA; 7.5 w/v% albumin D-PBS(-) solution, from bovine serum, Wako Pure Chemical Industries, Ltd., Osaka, Japan) at 37°C in a humidified 5% CO_2/95% air atmosphere for 1 h. The final concentration of each protein in the medium was 50 μg/cm^2 mucin, 10wt% FBS, 1 μg/cm^2 fibronectin, or 50 μg/cm^2 BSA. After the grooved composite resins were washed twice with fresh DMEM medium without serum, HGF was seeded at a density of 27,000 cells/cm^2 and incubated on pre-coated grooves for 1 h in DMEM without serum.

To assess the number of attached cells and cell alignment on the grooves, the attached cells were observed using an optical microscope and by SEM [15, 16]. After incubation, the grooves were rinsed with PBS to remove the non-adhering cells, fixed with a solution of 2.5% glutaraldehyde, and then stained with Giemsa dye. Cell attachment was evaluated from optical microscope images by counting the number of cells attached to each groove. Values represent the mean number and standard errors of the attached cells calculated from a 7-mm^2 field of each groove. The results are presented as the mean ± standard deviation of 6 experiments. For SEM observation, the grooves were rinsed with PBS to remove non-adhering cells, fixed with a solution of 2.5% glutaraldehyde, and then dehydrated in a graded series of alcohol (50%, 70%, 80%, 90%, 95%, and 100%) following critical-point drying. The grooved composite resin was coated by Pt-Pd sputtering. The morphology of attached cells on the grooves was observed using SEM.

D. Immunofluorescence staining

Immunofluorescence staining of the cells was carried out by a previously described method [17]. Briefly, after 1-h incubation, the attached cells were washed three times in PBS and fixed for 5 min in 4% paraformaldehyde in PBS. The cells were permeabilized with 0.5% Triton X-100 in PBS for 10 min and washed three times in PBS and blocked in 1% BSA for 30 min. After washing with PBS, the cells were incubated with 8 μl of anti-vinculin Alexafluor® 488 for vinculin fluorescence (0.5 mg/ml; eBioscience, San diego, CA, USA), 4 μl of Acti-stain^{TM} 555 fluorescent phalloidin (14 μM; Cytoskeleton Inc., Denver, CO, USA) for F-actin fluorescence, and 3 μl of DAPI solution (1 mg/ml; Dojindo Laboratories, Kumamoto, Japan) for nuclei fluorescence in 500 μl of PBS containing 1% BSA at 37°C for 1h and followed by incubation at 4°C overnight. Finally, the specimen was then washed three

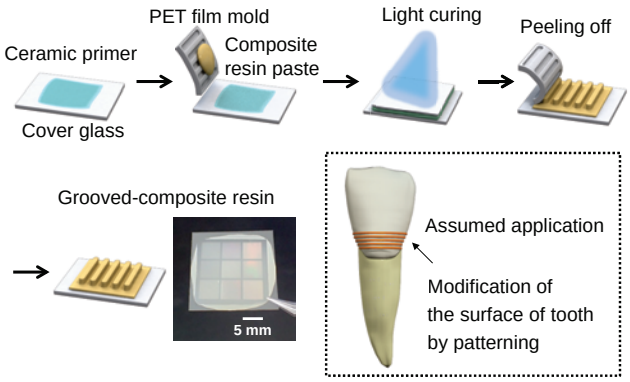

FIG. 1. Preparation of micro/nano-grooved composite resin and assumed application for surface modification of tooth by patterning.

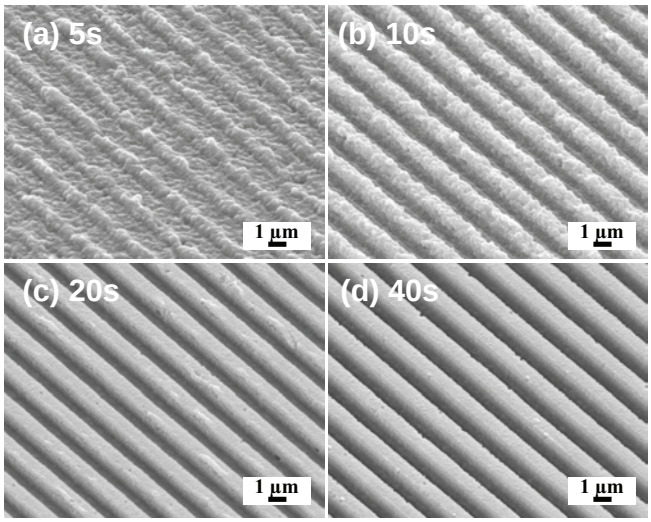

FIG. 2. Effect of irradiation time of light-curing on surface morphology of grooved composite resin. Irradiation time is (a) 5 s, (b) 10 s, (c) 20 s, and (d) 40 s. Groove mold size was a width of 0.5 μm and height of 1 μm.

times in PBS and mounted with fluoro-KEEPER antifade reagent (non-hardening type; Nacalai Tesque, Inc., Kyoto, Japan) and observed with a fluorescence microscope (BZ-9000; Keyence Corp., Osaka, Japan).

E. Statistical analysis

Statistical analysis was performed using GraphPad Prism version 6.05 (GraphPad Software, Inc., La Jolla, CA, USA). All data are presented as the mean ± standard deviation. Statistical differences were analyzed by unpaired t test. A value of $p < 0.05$ was considered statistically significant.

III. RESULTS AND DISCUSSIONS

A. Preparation of grooved composite resin

We prepared micro/nano-scaled grooves with composite resins by light-curing a flowable composite resin using a G-PET replica mold. The procedure is illustrated in Fig. 1. G-PET was selected as the replica mold because of its flexibility, easy preparation of replicas, and oxygen barrier property. SEM images of the patterns revealed the effect of irradiation time on the surface morphology of composite resins (Fig. 2). Although obscure groove shapes were observed at 5 and 10 s curing, clear groove shapes corresponding to the mold were observed at 20 and 40 s curing. Therefore, the composite resin can be cured at 20 s. Using a silicone mold rather than G-PET, the surface of composite resin did not cure because of its oxygen permeability (data not shown). Thus, the oxygen barrier property of the G-PET mold is effective for radical polymerization at the surface of the composite resin. Figures 3(a)-3(c) show the SEM images of grooved composite resins with different widths. Pattern shapes with a width between 2 μm and 500 nm exhibited clear groove shapes. Thus, this method can be applied for small grooves of at least 500 nm. Figures 3(d) and 3(e) show the laser microscope image and sectional analysis of 1-μm grooves. R_a value of 1-μm grooves was 0.44 ± 0.01 μm. Sectional

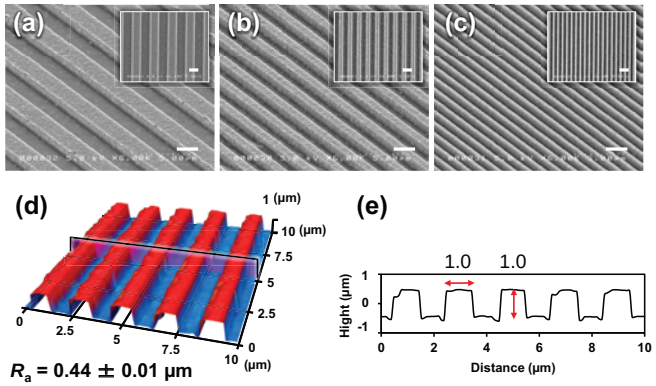

FIG. 3. SEM images of micro/nano-grooved composite resins irradiated for 20 s. Groove has a width of 2 μm (a), 1 μm (b), and 500 nm (c) and height of 1 μm. Insets shows top-view images of the groove surface. Scalebar = 2 μm. Laser microscope images of grooved composite resin irradiated for 20 s. Surface topography and roughness R_a (d) and sectional analysis (e) of groove with a width of 1 μm and height of 1 μm.

analysis of the grooves revealed that they were 1.0 μm in both width and height. Shrinkage of the composite resin was not observed. Thus, the resulting groove shapes corresponded to the groove shapes of the mold. Our results for the fine transfer property by patterning using flowable composite resin were similar to those of Frenzel *et al.* [14]. Dental flowable composite resin is suitable for patterning with micro/nano sized molds because of its high flow properties.

B. Attachment of HGF on mucin-coated grooves

As grooved composite resins are used in the oral environment, cell attachment to the surface of grooved composite resins may be blocked by saliva-coating [12]. Mucin

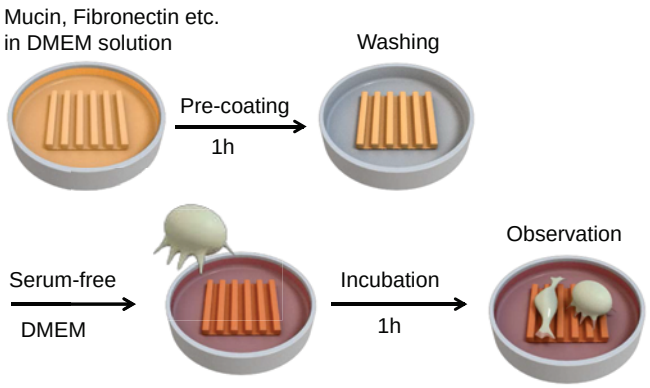

FIG. 4. Cell attachment assay of HGF on grooved composite resins. Groove has a diameter of 1 μm and height of 1 μm. (a) pre-coating, (b) washing, (c) incubation in serum-free medium, and (d) observation of cell attachment and alignment.

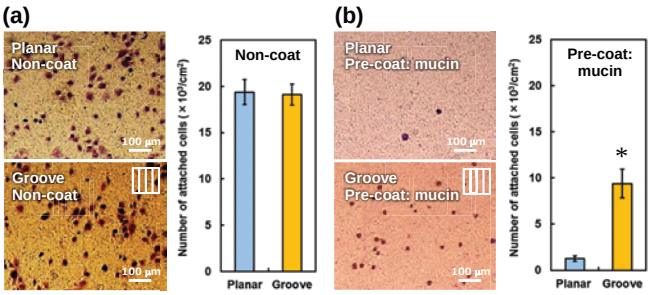

FIG. 5. Effect of pre-coating of mucin on attachment of HGF on grooved composite resin. Groove with a diameter of 1 μm and height of 1 μm was used. The groove was pre-coated with mucin; HGF was incubated on the groove in serum-free medium for 1 h. Insets indicate groove direction. Statistical difference was analyzed by unpaired t test (* indicates $p < 0.05$).

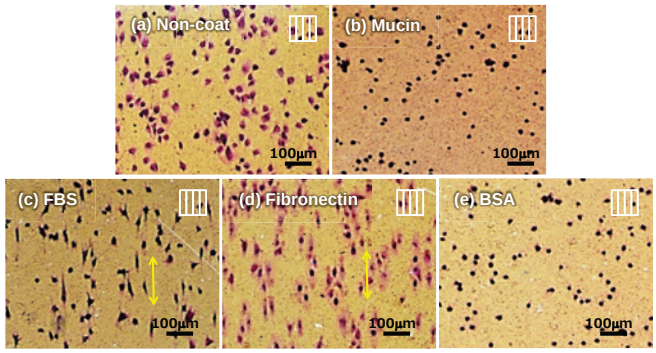

FIG. 6. Effect of pre-coating on alignment of HGF on grooved composite resins. Groove has a diameter of 1 μm and height of 1 μm. HGF was incubated for 1 h. Pre-coated substance (pre-coating concentration in DMEM); (a) non (0%), (b) mucin (50 μg/cm^2), (c) FBS (10 wt%), (d) fibronectin (1 μg/cm^2), and (e) BSA (50 μg/cm^2). Insets indicate groove direction.

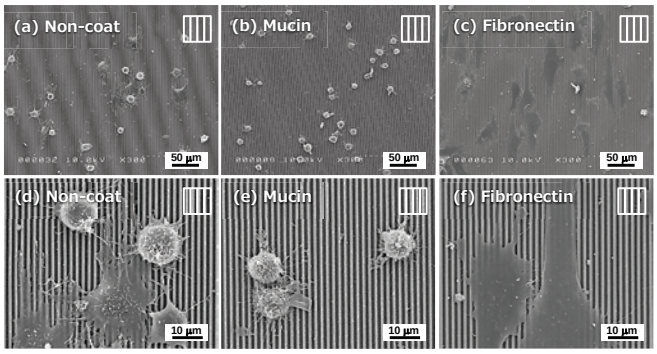

FIG. 7. SEM images of attached cells of HGF on pre-coated grooved composite resins. Groove has a diameter of 1 μm and height of 1 μm. HGF was incubated for 1 h. Pre-coating proteins (pre-coating concentration in DMEM) were (a and d) non (0%), (b and e) mucin (50 μg/cm^2), and (c and f) fibronectin (1 μg/cm^2). Insets indicate groove direction.

acts as a viscoelastic lubricant that coats all surfaces in the oral environment [18]. Thus, easily obtainable mucin was selected as the pre-coating protein rather than saliva in this study. To estimate the cell attachment ability of grooved composite resins, we carried out cell attachment assays of pre-coated grooves using HGF under serum-free conditions (Fig. 4). Figure 5(a) shows the number of attached cells to the planar or grooved composite resins after 1-h incubation. The graph shows that a similarly large number of cells attached to both composite resins ($p > 0.05$). The optical microscope images of cells revealed a large area and spreading in all directions. These results indicate strong adhesion behavior under serum-free conditions because of the high hydrophobicity of composite resins.

Figure 5(b) shows that the number of attached cells on both composite resins was lower than those without pre-coating were. Their morphology had a small area and round shape. Decreasing HGF attachment on the planar or grooves pre-coated with mucin agrees with the decreased HGF cell attachment to polystyrene coated with mucin or whole human saliva described previously [19]. Mucin may block cell attachment because of its heavily glycosylated glycoproteins. Interestingly, the number of attached cells on grooves pre-coated with mucin was 5.7-fold higher than that on planar pre-coated with mucin was, as shown in Fig. 5b ($p < 0.05$). Grooves at the micro/nano level may have acted as a hook for floating cells during the cell attachment assay.

C. Alignment of HGF on pre-coated grooves

To estimate the effect of protein adsorption on cell alignment, we carried out a cell attachment assay of HGF on grooves that had been pre-coated with some proteins (Fig. 4). Figure 6 shows the optical microscope images of cells attached to the grooves pre-coated with mucin, FBS, fibronectin, or BSA after 1-h incubation. The degree of cell alignment was strongly dependent on the pre-coating protein types. Cells on non-coated grooves exhibited large areas and radial spreading (Fig. 6(a)). Furthermore, SEM images revealed that the cells were radially spread or round, but did not sufficiently align with the

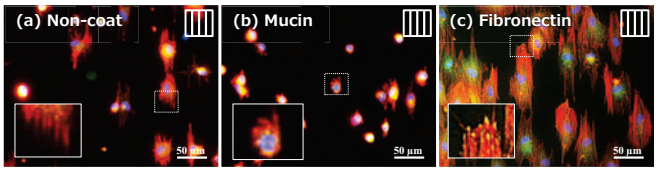

FIG. 8. Immunofluorescence images of attached cells of HGF on pre-coated grooved composite resins. Groove has a diameter of 1 μm and a height of 1 μm. HGF was incubated for 1 h. Pre-coating proteins (pre-coating concentration in DMEM) were (a) non (0%), (b) mucin (50 μmg/cm^2), and (c) fibronectin (1 μg/cm^2). Insets on the top of right indicate groove direction. Green: vinculin, Red: F-actin, and Blue: nuclei.

non-coated grooves (Figs. 7(a) and 7(d)). In a serum-free medium, non-coated composite resin showed a strong cell attachment ability because of the strong hydrophobicity of composite resin. Although the cells attached to the grooves, they were not aligned along the direction of the grooves. SEM images revealed that a part of the filopodia from the cell body was aligned along the direction of the grooves (Fig. 7(d)). This disregarded alignment of gingival fibroblast cells on composite resign grooves in serum-free conditions was similar to the decreasing percentage of aligned cells using epithelial cells on wafer grooves that were 0.4–2 μm width and under serum-free conditions [10]. Figure 8(a) shows immunofluorescence image of the attached cells on non-coated grooves. Some of cells were a little extended. Their F-actins were aligned in the groove direction, whereas vinculin spots were not observed as shown in Fig. 8(a) magnified inset. It seems to be difficult for the body of cells to extend along grooves. Therefore it is thought that cell alignment is considerably slower in serum-free medium.

The cells on grooves pre-coated with mucin or BSA covered a small area and were round (Figs. 6(b) and 6(e)). The cells extended some filopodia and gripped the mucin-coated grooves, but the cells did not align along the grooves (Fig. 7(b) and 7(e)). The cells were round shape and not largely expanded in Fig. 8(b). Good alignment of F-actin and vinculin spot of the cells were not observed in Fig. 8(b) magnified inset. BSA blocks cell adhesion or protein adsorption. Mucin functions as a lubricant in the oral environment [16]. Thus, pre-coating with mucin or BSA inhibited cell spreading and alignment. Furthermore, the number of attached cells on the planar pre-coated with mucin was considerably lower than that on grooves pre-coated with mucin (Fig. 5(b)). Therefore, the patterning of composite resin can improve cell attachment blocked by saliva contamination in the oral cavity.

Cells on FBS- or fibronectin-coated grooves exhibited good alignment in the groove direction, with particularly strong alignment observed on fibronectin-coated grooves (Figs. 6(c) and 6(d)). Nearly all cells on fibronectin-coated grooves were aligned and showed large spreading areas over some grooves (Figs. 7(c) and 7(f)). F-actins of most cells were aligned in the groove direction in Fig. 8(c). Furthermore, vinculin spots, indicating strong adhesion, in some cells were observed as shown in Fig. 8(c) magnified inset. Previous studies reported alignment of MG-63 cells [8], HGFs [20], dermal fibroblasts [9], epithelial cells [21], HeLa cells, and NIH/3T3 cells [22] on fibronectin-coated grooves. First, the filopodia of attached cells recognized the RGD sequence of fibronectin adsorbed to the ridge surface in the groove/ridge structure. Next, the attached cells form focal adhesions on the edge of the ridge, and then generate actin filaments aligned along the direction of the grooves [8]. Under typical culture conditions, cell alignment was also observed in medium supplemented with FBS. Fibronectin is known as an extracellular adhesion molecule in FBS and is a key component for cell attachment and cell alignment on the grooves.

IV. CONCLUSIONS

We prepared composite resins with grooves that had widths of 2 μm, 1 μm, and 500 nm and estimated the effect of pre-coating with various proteins on attachment and alignment of HGFs. The cells on grooves pre-coated with mucin covered a small area and were round, but the cells did not align along the grooves. Furthermore, the number of cells attached on the grooves pre-coated with mucin was considerable higher compared to that of planar pre-coated with mucin. Therefore, patterning of composite resin can improve cell attachment in mucin solution. However, bacterial adhesion may be promoted on grooved composite resins [14]. It may be necessary to use antibacterial agents mixed with grooved composite resin. Furthermore, our patterning method can be used to effectively seal the soft tissue and dental materials to protect against microorganism invasion [20, 23]. In the future, we will apply the surface modification of the tooth by pattering the seal between composite resin and soft tissue (Fig. 1).

ACKNOWLEDGMENTS

This work was partly funded by the “Adaptable and Seamless Technology Transfer Program through Target-driven R&D” Grant Number(No. AS251Z00599P) from the Japan Science and Technology (JST), by Suharakinenzaidan Co., Ltd., and by JSPS KAKENHI Grant Number(No. 25463047). The surface topographic analysis and sectional analysis of patterns were carried out using a 3D laser scanning confocal microscope (VK-X200) at the OPEN FACILITY, Hokkaido University Sousei Hall.

[1] E. Ercan, C. Candirli, T. Arin, L. Kara, and C. Uysal, Laser Med. Sci. **30**, 11 (2015).

[2] G. E. Pecora, R. Ceccarelli, M. Bonelli, H. Alexander, and J. L. Ricci, Implant Dent. **18**, 57 (2009).

[3] R. A. Delgado-Ruíz, J. L. Calvo-Guirado, P. Moreno, J. Guardia, G. Gomez-Moreno, J. E. Mate-Sánchez, P. Ramirez-Fernández, and F. Chiva, J. Biomed. Mater. Res. B Appl. Biomater. **96**, 91 (2011).
[4] M. S. Laranjeira, Â. Carvalho, A. Pelaez-Vargas, D. Hansford, M. P. Ferraz, S. Coimbra, E. Costa, A. Santos-Silva, M. H. Fernandes, and F. J. Monteiro, Sci. Technol. Adv. Mater. **15**, 025001 (2014).
[5] D. Nadeem, T. Sjostrom, A. Wilkinson, C.-A. Smith, R. O. C. Oreffo, M. J. Dalby, and B. Su, J. Biomed. Mater. Res. A **101**, 3247 (2013).
[6] R. G. Flemming, C. J. Murphy, G. A. Abrams, S. L. Goodman, and P. F. Nealey, Biomaterials **20**, 573 (1999).
[7] A. I. Teixeira, G. A. Abrams, P. J. Bertics, C. J. Murphy, and P. F. Nealey, J. Cell Sci. **116**, 1881 (2003).
[8] W. B. Tsai, Y. C. Ting, J. Y. Yang, J. Y. Lai, and H. L. Liu, J. Mater. Sci. Mater. Med. **20**, 1367 (2009).
[9] E. T. den Braber, J. E. de Ruijter, L. A. Ginsel, A. F. von Recum, and J. A. Jansen, J. Biomed. Mater. Res. **40**, 291 (1998).
[10] R. Amid, M. Torshabi, K. Tabari, M. Kadkhodazadeh, S. Eslami, and M. G. Ahsaie, J. Peridontal. Implant Dent. **8**, 24 (2016).
[11] S. Imazato, D. Horikawa, K. Ogata, Y. Kinomoto, and S. Ebisu, J. Biomed. Mater. Res. A **76**, 765 (2006).
[12] M. Koppolu, D. Gogala, V. B. Mathew, V. Thangala, M. Deepthi, and N. Sasidhar, J. Conserv. Dent. **15**, 270 (2012).
[13] R. J. Gibbons, J. Dent. Res. **68**, 750 (1989).
[14] N. Frenzel, S. Maenz, V. S. Beltrán, A. Völpel, M. Heyder, B. W. Sigusch, C. Lüdecke, and K. D. Jandt, Dent. Mater. **32**, 476 (2016).
[15] T. Akasaka, A. Yokoyama, M. Matsuoka, T. Hashimoto, S. Abe, M. Uo, and F. Watari, Bio-Med. Mater. Eng. **19**, 147 (2009).
[16] T. Akasaka, H. Miyaji, N. Kaga, A. Yokoyama, S. Abe, and Y. Yoshida, Nano Biomedicine **8**, (2016), in press.
[17] N. Kaga, T. Akasaka, R. Horiuchi, Y. Yoshida, and A. Yokoyama, Nano Biomedicine **8**, (2016), in press.
[18] C. Dawes, A. M. L. Pedersen, A. Villa, J. Ekström, G. B. Proctor, A. Vissink, D. Aframian, R. McGowan, A. Aliko, N. Narayana, Y. W. Sia, R. K. Joshi, S. B. Jensen, A. R. Kerr, and A. Wolff, Arch. Oral Biol. **60**, 863 (2015).
[19] M. O. Gabriel, T. Grünheid, and A. Zentner, J. Periodontol. **76**, 1175 (2005).
[20] Y. Lai, J. Chen, T. Zhang, D. Gu, C. Zhang, Z. Li, S. Lin, X. Fu, and S. Schultze-Mosgau, J. Dent. **41**, 1109 (2013).
[21] V. Raghunathan, C. McKee, W. Cheung, R. Naik, P. F. Nealey, P. Russell, and C. J. Murphy, Tissue Eng. Part A **19**, 1713 (2013).
[22] X. Zhou, J. Shi, J. Hu, and Y. Chen, Mater. Sci. Eng. C **33**, 855 (2013).
[23] M. Welander, I. Abrahamsson, and T. Berglundh, Clin. Oral Implants Res. **19**, 635 (2008).